PHYSOR 2004 -The Physics of Fuel Cycles and Advanced Nuclear Systems: Global Developments
Chicago, Illinois, April 25-29, 2004, on CD-ROM, American Nuclear Society, Lagrange Park, IL. (2004)

Evaluation of Turbulence Models for Flow and Heat Transfer in Fuel Rod Bundle Geometries

T. Sofu[*1], T. H. Chun[2], and W.K. In[2]
[1]*Argonne National Laboratory, 9700 S. Cass Ave., Argonne, IL 60439 USA*
[2]*Korea Atomic Energy Research Institute, Yusung, Daejeon 305-600, Korea*

One of the objectives of the US-ROK collaborative I-NERI project known as the "Numerical Reactor" is an assessment of commercial Computational Fluid Dynamics (CFD) analysis capabilities for high-fidelity thermal-hydraulic analysis of current and advanced reactor designs. More specifically, the work involves evaluation of common turbulence models in terms of their ability to calculate the flow and heat transfer for simple fuel rod bundle configurations. The evaluations have so far focused mostly on Reynolds-Averaged Navier-Stokes (RANS) models--including the standard k-ε model, non-linear (quadratic and cubic) k-ε models, and the renormalization-group (RNG) variant. The second-order moment closure models such as the differential Reynolds stress model (RSM) have also been considered.

KEYWORDS: CFD, turbulence models, Reynolds-Averaged Navier-Stokes models

1. Introduction

As part of the development effort on a whole-core analysis capability for integrated simulation of neutronic, thermal-hydraulic, and thermo-mechanical phenomena, the computational fluid dynamics (CFD) methods are considered to calculate flow and heat transfer in fuel-assemblies.[1,2] This integrated simulation capability departs from the conventional coupled neutronic/thermal-hydraulic model development efforts through rigorous pin-by-pin representation of fuel assemblies and surrounding coolant channels in the core. The separate-effects assessments of the reactor physics and thermal-hydraulics modules are being performed via cross-code evaluations or comparisons with experimental data. In the thermal-hydraulics area, the efforts have so far focused on the assessment of commonly used turbulence models for prediction of flow and heat-transfer in rod-bundle configurations.

A highly refined CFD model with the ability to resolve the effects of grid spacers can improve the accuracy of core design. While most commercial CFD software have the relevant capabilities needed in a reactor application, a demonstration of their ability to predict observed flows in rod bundle geometries is considered to be critical for their inclusion in the integrated code system. In this work, many widely used CFD software, including STAR-CD, CFX, FLUENT, FIDAP, CFD-ACE, and FLOTRAN are considered, and their specific capabilities relevant to the integrated simulation of a reactor core are reviewed. These capabilities include turbulent flow models, conjugate transfer, transient analysis, multi-phase flow, moving boundary, fluid-structure interactions, and parallel computing. More detailed evaluations were performed with STAR-CD, CFX, and CFD-ACE codes, mostly based on their availability at ANL and KAERI.

[*] Corresponding author, Tel. 630-252-9673, E-mail: tsofu@anl.gov

Independently, an evaluation of CFD turbulence models was initiated at ANL and KAERI for modeling turbulent flow in fuel rod bundle geometries.[3,4] More recently, these evaluations were extended to include additional configurations, such as flow in a bundle with a mixing promoter, and modeling of turbulent heat transfer. The evaluations focused mostly on Reynolds-Averaged Navier-Stokes (RANS) models. The most commonly known RANS models include the standard high Reynolds number k-ε model, non-linear (quadratic and cubic) k-ε models, low Reynolds number k-ε model, and the renormalization-group (RNG) variant. The second-order moment closure models and combination of low and high Reynolds number models (double layer approach) have also been evaluated. Since the two-phase flow simulation capabilities of the current generation CFD codes are rather limited, the assessments have so far focused on single-phase flow and heat transfer.

2. Description of RANS Models

Solving Navier-Stokes equations for mass, momentum, and energy conservation to simulate flow and heat transfer in a reactor core provides a mechanistic approach based on first-principles. For turbulent flows, the field variables and Reynolds stresses assume their ensemble averaged values that are linked to the mean flow field via turbulence closure models that comprise a set of additional differential or algebraic equations. The most commonly used turbulence models fall under the category of Reynolds Averaged Navier-Stokes (RANS) models. And the most widely known RANS models are the k-ε models based on solving two additional differential transport equations for the turbulence energy, k, and its rate of dissipation, ε. The standard k-ε model[5] is based on solving the high Reynolds number forms of the k and ε equations using a linear eddy viscosity hypothesis for the Reynolds stresses

$$\tau_{ij} = -\rho\overline{u_i' u_j'} = \mu_t\left(\frac{\partial U_i}{\partial x_j} + \frac{\partial U_j}{\partial x_i}\right) - \frac{2}{3}\rho k\delta_{ij}$$

where the turbulent viscosity is given by

$$\mu_t = \rho C_\mu \frac{k^2}{\varepsilon}.$$

Most often, the standard k-ε model is used in conjunction with algebraic "wall-functions" that represent flow and heat transfer within the boundary layers. A low Reynolds number variant of the k-ε model[6] is based on solving the transport equations for k and ε for the entire computational domain including the boundary layers, assuming low-power and low-flow conditions in the core. A more computation intensive option is the two-layer approach[7] based on solving the high Reynolds number forms of the k and ε equations in combination with the low Reynolds number forms to resolve the boundary layer.

The anisotropic eddy viscosity relationship removes the assumption of turbulence isotropy by formulating a constitutive relation for the Reynolds stresses resulting in a finite tensor polynomial. The non-linear k-ε models are based on quadratic[8-10] and cubic[11] constitutive relations for the Reynolds stresses expressed respectively as

$$\rho\overline{u_i' u_j'} = -\mu_t S_{ij} + \frac{2}{3}\rho k\delta_{ij} + C_1\mu_t\frac{k}{\varepsilon}\left(S_{ik}S_{kj} - \frac{1}{3}S_{kl}S_{kl}\delta_{ij}\right) + C_2\mu_t\frac{k}{\varepsilon}\left(\Omega_{ik}S_{kj} + \Omega_{jk}S_{ki}\right)$$
$$+ C_3\mu_t\frac{k}{\varepsilon}\left(\Omega_{ik}\Omega_{jk} - \frac{1}{3}\Omega_{lk}\Omega_{lk}\delta_{ij}\right)$$

$$\rho\overline{u_i'u_j'} = -\mu_t S_{ij} + \frac{2}{3}\rho k\delta_{ij} + C_1\mu_t\frac{k}{\varepsilon}\left(S_{ik}S_{kj} - \frac{1}{3}S_{kl}S_{kl}\delta_{ij}\right) + C_2\mu_t\frac{k}{\varepsilon}\left(\Omega_{ik}S_{kj} + \Omega_{jk}S_{ki}\right)$$
$$+ C_3\mu_t\frac{k}{\varepsilon}\left(\Omega_{ik}\Omega_{jk} - \frac{1}{3}\Omega_{lk}\Omega_{lk}\delta_{ij}\right) + C_4\mu_t\frac{k^2}{\varepsilon^2}\left(S_{ki}\Omega_{lj} + S_{kj}\Omega_{li}\right)S_{kl}$$
$$+ C_5\mu_t\frac{k^2}{\varepsilon^2}\left(\Omega_{il}\Omega_{lm} + S_{il}l\Omega_{lm}\Omega_{mj} - \frac{2}{3}S_{lm}\Omega_{mn}\Omega_{nl}\delta_{ij}\right) + C_6\mu_t\frac{k^2}{\varepsilon^2}S_{ij}S_{kl}S_{kl} + C_7\mu_t\frac{k^2}{\varepsilon^2}S_{ij}\Omega_{kl}\Omega_{kl}$$

where the non-dimensional strain rate and vorticity are given, respectively, by

$$S_{ij} = \left(\frac{\partial U_i}{\partial x_j} + \frac{\partial U_j}{\partial x_i}\right) \quad \text{and} \quad \Omega_{ij} = \left(\frac{\partial U_i}{\partial x_j} - \frac{\partial U_j}{\partial x_i}\right) - \varepsilon_{ijk}\Omega_k .$$

Other variations of RANS models include the renormalization group (RNG) version[12] and Chen's variant.[13] The more complex second-order closure models such as the differential Reynolds Stress Model (RSM) [14] based on exact transport equations for the individual Reynolds stresses as derived from the Navier-Stokes equations are also considered. While the common empirical coefficients appearing in these closure models are part of the turbulence approximations (and some of them are functions of other variables themselves), these models are believed to be applicable to a fairly broad class of flow and heat transfer regimes for a wide range of fluids.

3. Turbulence Model Assessments

3.1 Analysis of Isothermal Flow Through a Square Rod Bundle

Initially, numerical simulation of turbulent flow structure has been performed at KAERI for a square bare rod bundle.[15] Assuming flow symmetry, an octant subchannel is modeled with a 25x50 computational grid in radial and azimuthal directions as shown in Figure 1. The calculations are performed at Re=207,600 for a pitch to diameter ratio of 1.107.

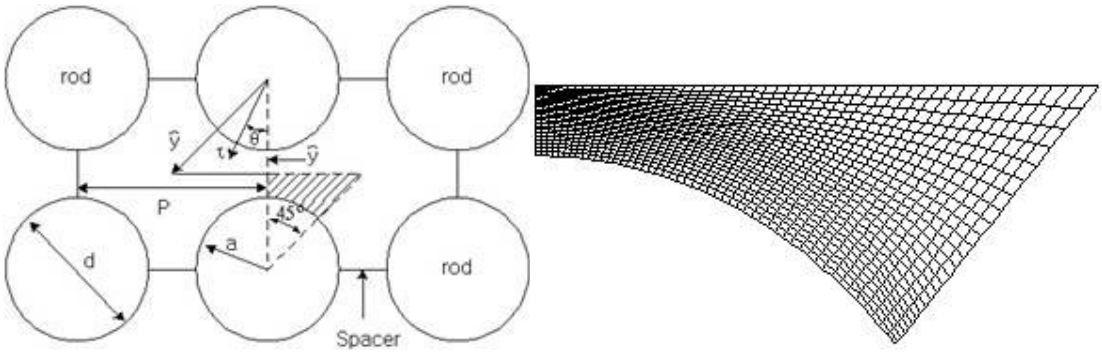

Figure 1. Schematic of Square Rod Bundle and Computational Grid of Octant Subchannel.

The turbulence-driven secondary flows are captured with all non-linear RANS and RSM models, exhibiting a lateral counter-clockwise recirculation pattern in the subchannel caused by turbulence anisotropy (Figure 2). The maximum lateral speed for this secondary flow pattern is estimated to vary between 0.9% and 2.2% of the mean bulk velocity as shown in Figure 2. These predictions compare well with the measurements for a triangular bare rod bundle[16] which show a maximum lateral speed on the order of 1% of the mean bulk velocity.

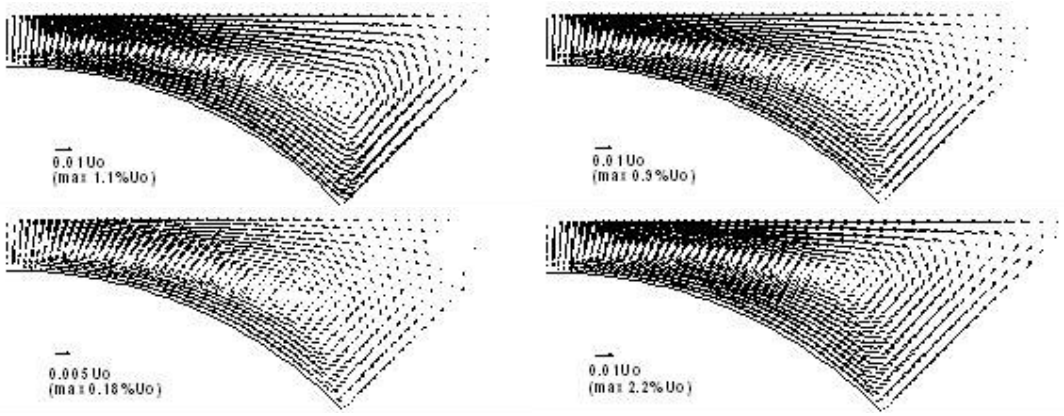

Figure 2. Turbulence-Driven Secondary Flow as Predicted by the Nonlinear Turbulence Models: (Clockwise from Top Left) Ref. 8, Ref. 9, Ref. 14, and Ref. 11.

On the other hand, the axial velocity distribution is consistently under-predicted along the gap (between the fuel pins at θ=0), and over-predicted along the diagonal (θ=45º) by all models as shown in Figure 3. The non-linear k-ε models provide more accurate predictions over the standard k-ε model; however, the best agreement with the experimental results is obtained with RSM.

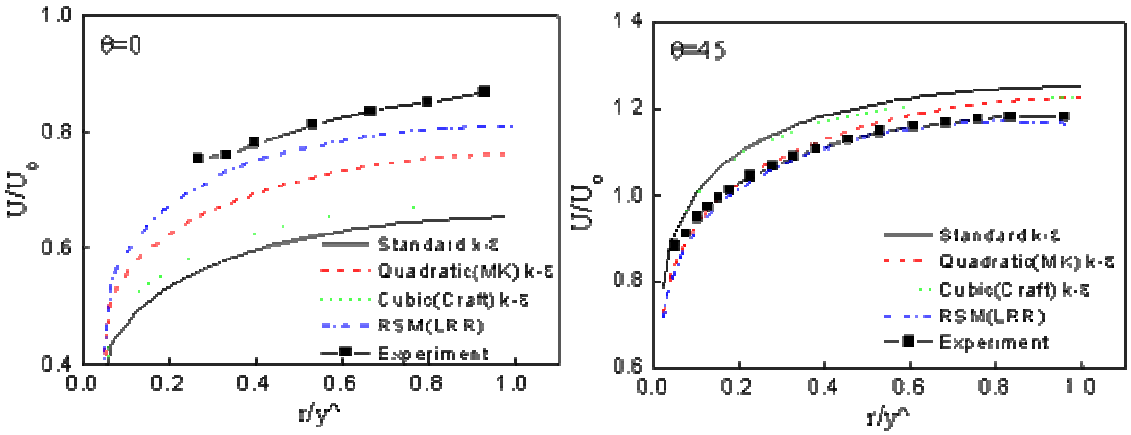

Figure 3. Mean Axial Velocity Distributions along the Gap (θ=0º) and along the Diagonal (θ=45º).

The radial variations of turbulence intensities are also compared with experimental data along the gap and along the diagonal as shown in Figure 4. The symbols u', v', w' in Figure 4 indicate axial, radial and azimuthal turbulence intensities, and they are normalized with respect to the friction velocity u_τ. The RSM predictions of v' and w' along the diagonal (θ=45º) are in good agreement with the measured values. The quadratic k-ε model predicts somewhat higher azimuthal intensity than the radial intensity. While the experimental data indicates significant increase in the azimuthal turbulence (w'>u') along the gap (θ=0º), the predicted values (the green curves) are considerably lower than the measured ones.

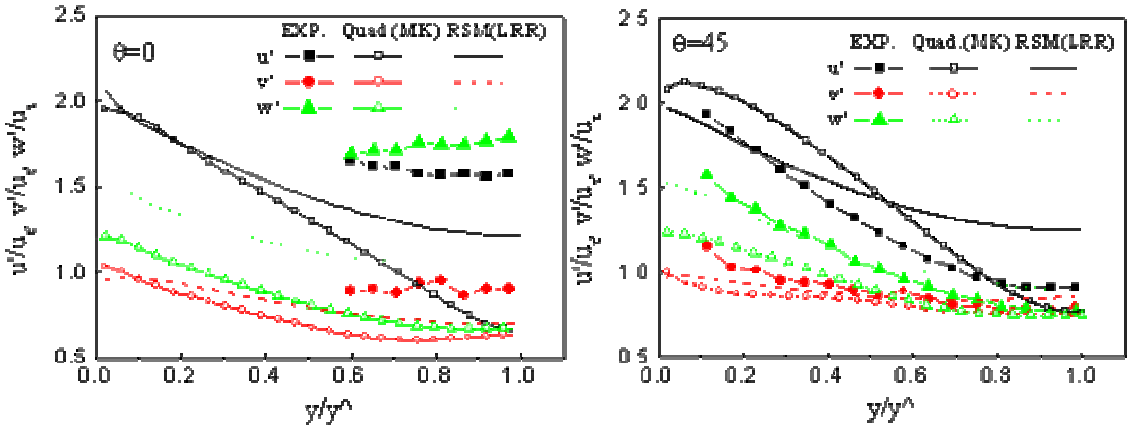

Figure 4. Comparisons of Turbulence Intensities along the Gap (θ=0º) and the Diagonal (θ=45º).

3.2 Heat Transfer Predictions for Flow in a Pipe

Because of limited experimental data available for turbulent heat transfer in rod bundles, the RANS-based turbulence models have been first assessed at ANL for heat transfer in a pipe (with an equivalent hydraulic diameter of a typical PWR flow channel), and compared to the values predicted with the well-known Dittus-Boelter correlation: $h_{DB}=(k/d)\cdot 0.023\cdot Re^{0.8}\cdot Pr^{0.4}$. [17] The flow parameters are set to values that are typical for a PWR operating at 5% to full-power with corresponding Re numbers ranging from 25,000 to 500,000. The heat transfer coefficient computed at the wall by the standard k-ε model on the basis of the bulk coolant temperature (h_{CFD}) is compared with the heat transfer coefficient computed by the Dittus-Boelter correlation (h_{DB}) in Figure 5 for several cases with constant power to flow ratio. The discrepancy between the computed and empirical values varies between 4% and 11%.

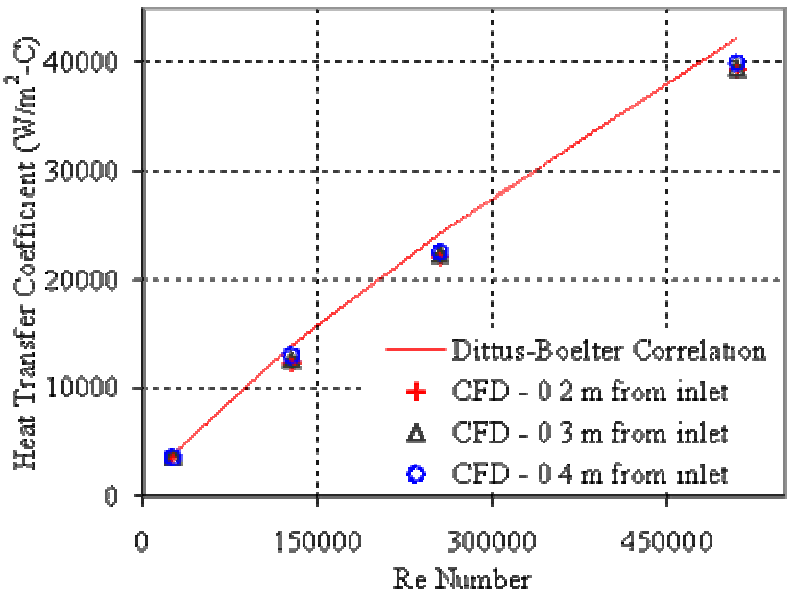

Figure 5. Heat Transfer Coefficient Comparisons with the Standard k-ε Model.

Analyses have also been repeated with the RNG and a two-layer models for the case of Re=254,809. In the two-layer model, the high Re number k-ε model is applied everywhere except a near-wall region where a low Reynolds number model is specified using a fine grid with non-dimensional thickness of near wall layer yielding $y^+=1$. In the near wall region, the distribution of ε was obtained from an algebraic function and the turbulent viscosity was dampened as provided by the Norris and Reynolds model.[18] A comparison of the results from the high Re number, the RNG, and the two-layer k-ε models are presented in Table 1. The comparison of the results with empirical values shows 3.5% discrepancy with two-layer model, 9% with the high Re number model, and 17% with the RNG model, suggesting that the fine resolution of the boundary layer results in substantial improvement in heat transfer predictions. Nevertheless, most RANS models, including the standard high Re number k-ε model provide predictions within the experimental uncertainty of the Dittus-Boelter correlation (±10%).

Table 1. Heat Transfer Coefficient Comparisons at Re = 254,809

	Distance from inlet	h_{CFD} W/(m^{2}C)	h_{CFD}/h_{DB}
High Re# Model	0.20 m	22,096	0.917
	0.30 m	22,257	0.910
RNG Model	0.20 m	20,138	0.829
	0.30 m	20,300	0.836
Two-layer Model	0.20 m	23,434	0.965
	0.30 m	23,637	0.973

Because k-ε models use wall functions in the boundary layer, it is recommended that the distance to the wall of the center of cells adjacent to a wall should be between about $30<y^+<100$. To assess the sensitivity of model predictions to the size of the near wall cells, analyses were performed with three different cell sizes for the high Re number k-ε model. The results suggest that, for the range of distances considered, the predictions are nearly independent of the cell center distance to the wall.

3.3 Analysis of Turbulent Heat Transfer in Heated Rod Bundles

More recently, a study of turbulent transport of momentum and energy in heated rod bundles has been performed at KAERI [19] using an experiment with 37-pin triangular array[20] as shown in Figure 6. Two different pitch-to-diameter ratios (P/D=1.06 and 1.12) have been investigated at Re=39,000 (with corresponding wall heat flux of 980 W/m2), and at Re=65,000 (with corresponding wall heat flux of 1390 W/m2). Only the 1/6 symmetric segment of the central triangular subchannel has been modeled as shown in Figure 6.

The predictions of normalized time-averaged axial velocity contours along with the measurements are shown in Figure 7 for P/D=1.06. Consistent with the analysis of the configuration in Figure 1, the non-linear k-ε and RSM models provide more accurate velocity distributions than the standard k-ε model. The maximum lateral speed for the secondary flow pattern is estimated to be 1.0% of the mean bulk velocity with quadratic k-ε model and 0.7% with RSM, consistent with the measurements reported in Ref. 16. Figure 8 shows the normalized time-averaged fluid temperature contours for P/D=1.06. The predicted results show generally higher temperature gradients over the subchannel than the measurements, resulting in higher fluid temperatures along the gap. Nonetheless, the quadratic k-ε model and RSM improve the predictions of fluid temperature distributions relative to the standard k-ε model. As the rod gap increases, the turbulent models show better predictions. There are no particular difference in the trend of turbulence predictions among models between P/D=1.06 and P/D=1.12.

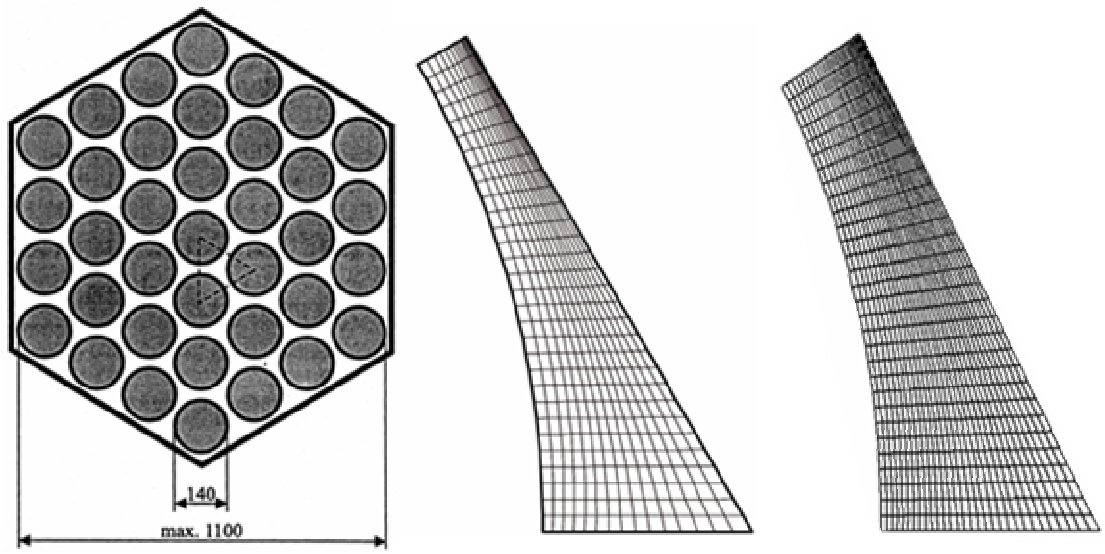

Figure 6. 37-rod heated bundle with triangular array, and the simulation grids for pitch-to-diameter ratio of 1.06 (middle) and 1.12 (right).

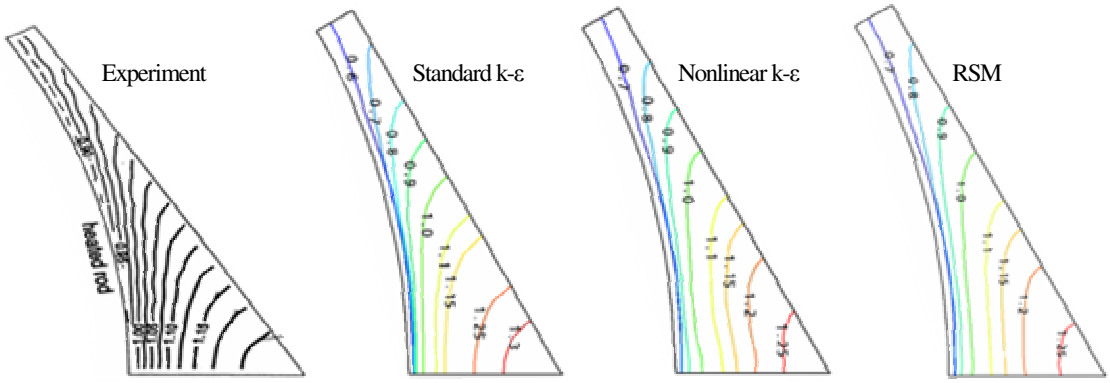

Figure 7. Distributions of mean velocity for P/D=1.06.

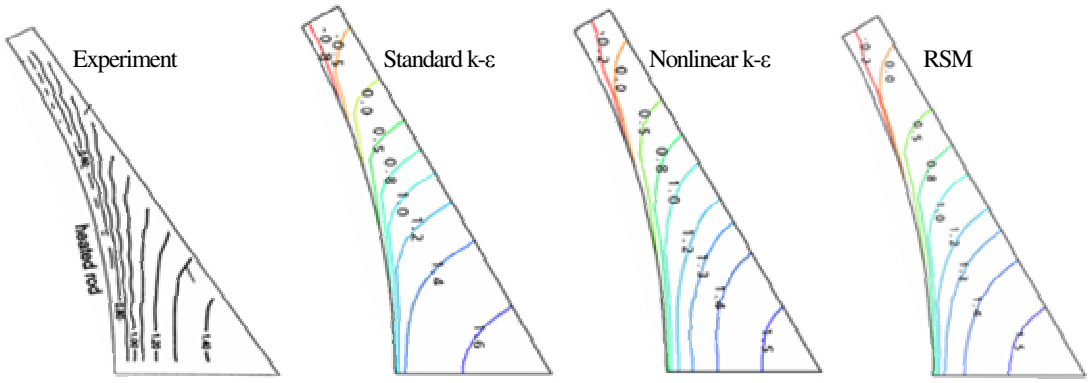

Figure 8. Time averaged temperature $((T_{w,m}-T)/(T_{w,m}-T_b))$ distributions for P/D=1.06.

Figure 9 compares the predicted normalized wall shear stresses along rod surface by turbulent models. The quadratic k-ε model and RSM reveal the maximum wall shear stress around θ=5º, which seems the effect of secondary flow. The measured shear stress distributions show rather mild variation along rod surface within ±15% and ±5% to the averages, respectively. Except the standard k-ε model, remaining turbulent models show similar predictions with reasonable accuracies. However, the prediction results get worse as P/D ratio decreases.

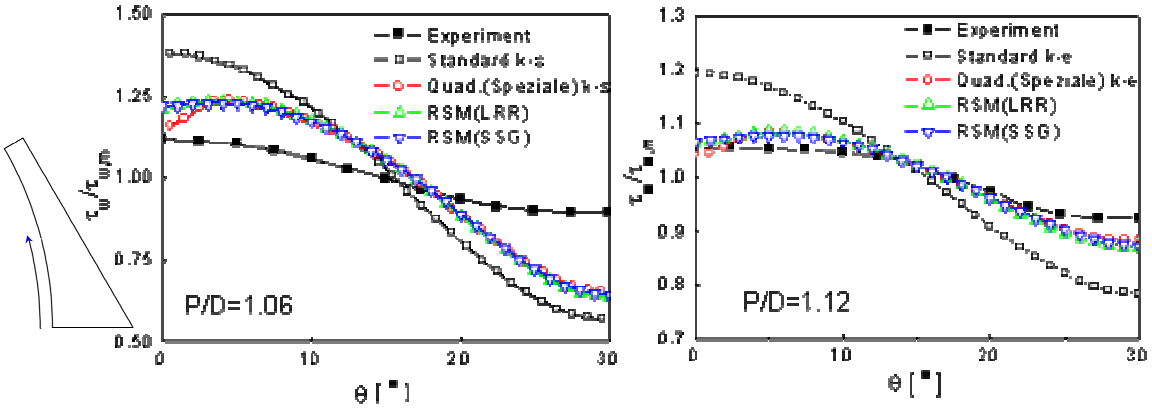

Figure 9. Normalized wall shear stress distributions.

Figure 10 shows the dimensionless wall temperature distribution along the rod surface $(T_w - T_{Ein})/T_{\tau,m}$, where $T_{\tau,m}$ is average wall friction temperature, T_w is local wall temperature, and T_{Ein} is inlet temperature. In general, the measured temperature distributions are quite uniform within 3%. But for narrow gap case (P/D=1.06), there are considerably large peripheral variations in predicted wall temperature distributions, particularly with the standard model relative to the measured values. However, for wider gap case (P/D=1.12), the predicted temperature distributions are closer to the measured values similar to the case with the wall shear stress distributions. It can be hypothesized that, when the rod gap gets narrower, a strong large eddy fluctuation takes over in the gap region between two adjacent rods, which is not properly captured with the RANS models.

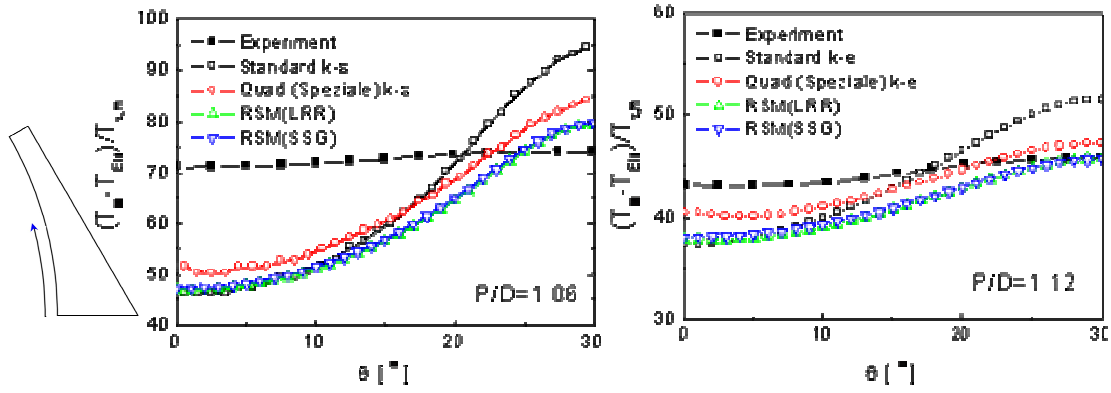

Figure 10. Distributions of dimensionless wall temperature.

4. Conclusions

The assessment of common turbulence models available in commercial CFD software have been conducted with mixed success. For a set of different rod bundle configurations with and without mixing promoters, the code predictions have been compared with data from literature on experiments with and without heat transfer. In general, the accurate predictions for distribution of turbulent structures in the subchannel have not been demonstrated with the most common standard k-ε model. However, the non-linear RANS models, RSM, and the double-layer approach based on the use of low-Re number k-ε model in the boundary layer seem to improve the predictions of turbulence intensity and fluid temperature distributions noticeably.

In summary, nonlinear quadratic k-ε model and RSM are considered more suitable to simulate the turbulent flow and heat transfer in bare rod bundle based on their ability to predict the turbulence-driven secondary flow properly. The comparisons also indicate a need for assessments of unsteady turbulence models like LES to simulate additional turbulent motion of large-scale eddy fluctuations of velocity and temperature near the narrow gap region, which is not formulated in existing RANS models.

Acknowledgements

This work was completed under the auspices of the U.S. Department of Energy Office of Nuclear Energy as part of the International Nuclear Energy Research Initiative (INERI) with Republic of Korea. The submitted manuscript has been created by the University of Chicago as Operator of Argonne National Laboratory ("Argonne") under Contract No. W-31-109-ENG-38 with the U.S. Department of Energy. The Korean side work was supported by the fund provided by the Ministry of Science and Technology of Korea.

References

1) D.P. Weber, et.al., "Integrated 3-D Simulation of Neutronic, Thermal-Hydraulic and Thermo-Mechanical Phenomena," Proc. 10th Intl. Topical Mtg. on Nuclear Reactor Thermal Hydraulics, NURETH-10, Seoul, Korea, October 5-9, 2003.
2) D.P. Weber, et.al., "The Numerical Nuclear Reactor for High Fidelity Integrated Simulation of Neutronic, Thermal-Hydraulic and Thermo Mechanical Phenomena," Proc. ANS Reactor Physics Topical Meeting, PHYSOR 2004, Chicago, Illinois, April 25-29, 2004.
3) C.P. Tzanos, "Computational Fluid Dynamics for the Analysis of Light Water Reactor Flows," Proc. 10th Intl. Topical Mtg. on Nuclear Reactor Thermal Hydraulics, NURETH-10, Seoul, Korea, October 5-9, 2003.
4) W.K. In, "Numerical Prediction of Flow in a Nuclear Fuel Bundle with Various Turbulence Models," Proc. Intl. ASME/JSME/KSME Symposium on CFD, Canada, 2002.
5) B.E. Launder and D.B. Spalding, "The Numerical Computation of Turbulent Flows," Computational Methods in Applied Mech. and Engineering, **3**, 269-289 (1974).
6) F.S. Lien, W.L. Chen, and M.A. Leschziner, "Low-Reynolds-Number Eddy-Viscosity Modelling Based on Nonlinear Stress-Strain/Vorticity Relations," Proc. 3rd Symp. on Eng. Turbulence Modeling and Measurements, Crete, Greece (1996).
7) W. Rodi, "Experience with Two-Layer Models Combining k-ε Model with a One-Equation Model Near the Wall," AIAA, 91-0216 (1991).

8) C. G. Speziale, "On Non-linear k-l and k-ε models of Turbulence," J. Fluid Mech., **178**, pp. 459-475 (1987).
9) H.K. Myong and N. Kasagi, "Prediction of Anisotropy of the Near Wall Turbulence with an Anisotropic Low-Reynolds-Number k-ε Turbulence Model," J. Fluids. Eng., **112**, pp. 521-524 (1990).
10) T. H. Shih, J. Zhu and J. L. Lumley, "A Realizable Reynolds Stress Algebraic Equation Model," NASA Tech. Memo 105993 (1993).
11) T.J. Craft, B.E. Launder and K. Sugar, "Development and Application of a Cubic Eddy-Viscosity Model of Turbulence," Int. J. Heat and Fluid Flow, **17**, pp. 108-115 (1996).
12) V. Yakhot and S.A. Orszag, "Renormalization Group Analysis of Turbulence—I: Basic Theory," J. Scientific Computing, **1**, pp. 1-51 (1992).
13) Y.S. Chen and S.W. Kim, "Computation of Turbulent flows using an extended k-ε turbulence closure model," NASA CR-179204 (1897).
14) B.E. Launder, G.J. Reece and W. Rodi, "Progress in the Development of a Reynolds Stress Turbulence Model," J. of Fluid Mech., **68**, pp. 537-566 (1975).
15) J.D. Hooper and D.H. Wood, "Fully Developed Rod Bundle Flow over a Large Range of Reynolds Numbers," Nucl. Eng. and Des., **83**, pp. 31-46 (1984).
16) V. Vonka, "Measurement of Secondary Flow Vortices in a Rod Bundle," Nucl. Eng. and Des., **106**, pp. 191-207, 1988.
17) F.W. Dittus and L.M.K. Boelter, Univ. of Calif. (Berkeley) Pub. Eng., 2, 443 (1930).
18) L.H. Norris and W.C. Reynolds, "Turbulent Channel Flow with a Moving Wavy Boundary," Report No.FM-10, Dept. of Mechanical Engineering, Stanford University, USA (1975).
19) W. K. In, C. H. Shin, D. S. Oh, T. H. Chun, "CFD Simulation of the Turbulent Flow and Heat Transfer in a Bare Rod Bundle," Proc. ICAPP'04 Pittsburgh, PA, June 13-17, 2004.
20) Krauss and Mayer, "Experimental investigation of turbulent transport of momentum and energy in a heated rod bundle," Nucl. Eng. and Des., **180**, 185-206 (1998).